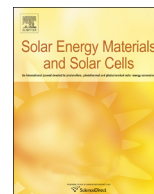




ELSEVIER

Contents lists available at ScienceDirect

Solar Energy Materials & Solar Cells

journal homepage: www.elsevier.com/locate/solmat

Pseudo-disordered structures for light trapping improvement in mono-crystalline Si thin-films



L. Lalouat^a, H. Ding^a, B. Gonzalez-Acevedo^a, A. Harouri^a, R. Orobtcchouk^a, V. Depauw^b,
E. Drouard^{a,*}, C. Seassal^a

^a Institut des Nanotechnologies de Lyon (INL), Université de Lyon, UMR5270, CNRS-INS-ECLE-UCBL Ecole Centrale de Lyon, 36 av. Guy de Collongue, Ecully 69134, France

^b Imec, Kapeldreef 75, Leuven B-3001, Belgium

ARTICLE INFO

Article history:

Received 15 July 2015

Received in revised form

22 February 2016

Accepted 15 April 2016

Available online 30 April 2016

Keywords:

Thin-film

Mono-crystalline silicon

Photonic crystal

Light trapping

ABSTRACT

Thin film solar cells may exhibit high conversion efficiencies provided their active material exhibits a high quality, like in the case of crystalline silicon, and if incident light coupling and absorption are appropriately controlled. We propose to integrate an advanced light trapping process relying on photonic crystals including a controlled pseudo-disorder. Thanks to Rigorous Coupled Wave Analysis, we determine the optimized nanophotonic structures that should be appropriately introduced in 1 μm thick crystalline silicon layers standing on a metal layer like aluminum. Thanks to a carefully controlled pseudo-disorder perturbation, absorption in these designed nanopatterns overcome that predicted in the case of fully optimized square lattice photonic crystals. Fabricated structures are analyzed in light of this numerical investigation to evidence the impact of such controlled perturbations, but also the influence of the measurement method and the technological imperfections. Thanks to the optimized perturbed photonic crystals, the integrated absorption in 1 μm thick crystalline Silicon layer increases from 37.7%, in the case of the unpatterned stack, to 70.7%. The sole effect of pseudo-disorder on the fully optimized simply periodic photonic crystals leads to an absolute increase of the integrated absorption up to 2%, as predicted by simulations, while both structures are fabricated using exactly the same process flow.

© 2016 Elsevier B.V. All rights reserved.

1. Introduction

Thin film solar cells using deposited material like hydrogenated amorphous silicon (a-Si:H) as an active material offer an alternative to photovoltaic (PV) devices made of bulk crystalline silicon (c-Si); they allow for cost reduction and specific characteristics like the integration on flexible modules, but generally at the expense of the conversion efficiency. Another approach consists in using a c-Si layer with a thickness in the 1–10 μm range. This is expected to lead to cost effective photovoltaic devices based on a high quality material, with reduced carrier bulk recombination. In order to achieve high conversion efficiency with such thin film c-Si solar cells, it is essential to optimize the incident light in-coupling and trapping in an otherwise relatively inefficient absorber, especially for long wavelength photons. Light trapping for photovoltaics has been a topic of strong interest in the past years, with the use of diffraction gratings [1], surface plasmons [2,3] or photonic crystals (PC) [4] in layers with thicknesses around 100 nm. Among all these

possibilities, photonic crystal structure is a promising route. Indeed, adding a periodic pattern in a thin film enables the conversion of out-of-plane wave-vectors into in-plane-wave-vectors results in an increase of the “effective” absorbing material thickness. Moreover, thanks to the periodicity of the photonic crystal, the dispersion law can be controlled to create slow Bloch modes guided into the thin film. Moving to higher quality materials, the theoretical absorption for a thin c-Si film over a broad wavelength range can be increased up to 50% when compared to the unpatterned case [5]. A few research groups recently demonstrated the operation of real solar cell devices, including such periodic nanophotonic structures within a solar cell based on c-Si layers. Among all the advances reported in this area, Chen et al. at MIT achieved a 15.7% efficiency with a 10 μm thick c-Si solar cell including periodic inverted pyramids [6]. Jeong at Stanford integrated nanocones structures on top of a 10 μm thick c-Si solar cells, leading to 13.7% efficiency [7], and PC patterning of a 1 μm thick c-Si layer on an aluminum back mirror leading to a J_{sc} of 15.4 mA/cm^2 , which corresponds to an increase of 20% compared to the unpatterned reference case [8]. Recently more complex structures that combine a front and a back photonic crystal structure [9–11] have been proposed to overcome this value by adding new optical modes

* Corresponding author.

E-mail address: Emmanuel.drouard@ec-lyon.fr (E. Drouard).

and/or tailoring the reflection at the bottom interface of the solar cell. Still, this approach is technologically quite complex, and the integration of an optimized and technologically feasible and cost effective light trapping strategy on a realistic solar cell stack has been barely addressed, in particular in the case of thin c-Si layers.

Due to the periodicity of the photonic crystal this approach is highly efficient only for specific wavelengths and angles as traduced by the high quality factor peaks obtained on a typical absorption spectrum. An alternative approach to this strictly periodic structuration that could decrease the coherence of the absorption processes is to use random structuration [12–14]. Such structures exhibit then rich Fourier spectra like the well-known quasi-crystal [15,16] that can also increase the absorption in a thin-film thanks to guided modes introduced by a rotational order that leads to an equivalent increase of 9% compared to a square lattice of holes for a 0.3 μm thick c-Si layer. As such structures are not deterministic, one may prefer to introduce a certain degree of disorder in the periodic pattern [17–20], to combine random fluctuations with a periodic pattern [21] or to use a binary grating approach [22]. In our approach, a supercell is made of randomly located holes periodically repeated in a square lattice in order to define a pseudo-disordered photonic crystal. Such an approach allows to quantify the magnitude of disorder introduced in an optimized nanopattern and to “engineer” the optical resonances related to the periodic pattern. Our approach was conducted on a technologically realistic thin photovoltaic stack. The thickness of the absorbing layer is chosen in order to eventually achieve a high absorption; of course, the absorption increase related to the photonic structure is then reduced compared to the case of an ultra-thin (< 500 nm) absorbing layer [16]. Lastly, our method relies on carefully positioned holes, in a way that can be achieved with a conventional lithography technique with a reduced effort compared to complex and very small patterns that have been proposed elsewhere [22]. Finally, to avoid additional surface passivation issues in the future development, keeping a lattice of cylindrical holes prevents any extra sidewall or nanopatterned shape differences, and enables to use the same conformal depositions conditions for the subsequent passivation of the nanopattern.

In this paper, we investigate numerically and experimentally the absorption in a thin c-Si structure patterned with a pseudo-disordered photonic crystal. More precisely, the stack under consideration is a 1 μm thick c-Si film bonded onto a 1 μm thick Al layer on a glass substrate as depicted in Fig. 1a. The Al layer acts as a back mirror, especially at the wavelengths above 0.5 μm where the single pass absorption in c-Si is low. It also acts as a back contact in a solar cell. A PC structure is then partially etched in the c-Si film, with a depth in the 100–200 nm range; it was shown elsewhere that such a design enables efficient in-coupling of the incident light into the pseudo-guided Bloch modes of the structure [5], leading to an efficient light trapping.

To establish a fair comparison, the integrated absorption of the sun light in the pseudo-disordered patterns is compared to the one of the perfect-square lattice of holes that maximizes the absorption in the same stack. It will be shown that the use of an optimized PC structure in front of our stack almost doubles the integrated absorption compared to the flat reference (a relative increase of 87.8% is obtained). Then, a pseudo-disordered PC, that can be realized in the same way as the optimized PC, can exhibit experimentally as well as theoretically a larger integrated absorption as the case of a square lattice of holes, at almost no extra technological cost.

Section 2 is dedicated to a numerical investigation on the effect of a controlled pseudo-disorder introduced in a periodic photonic crystal structure. The total absorption of the thin c-Si films on metal is numerically optimized using the Rigorous Coupled Wave Analysis (RCWA) method [23]. Let us underline that this

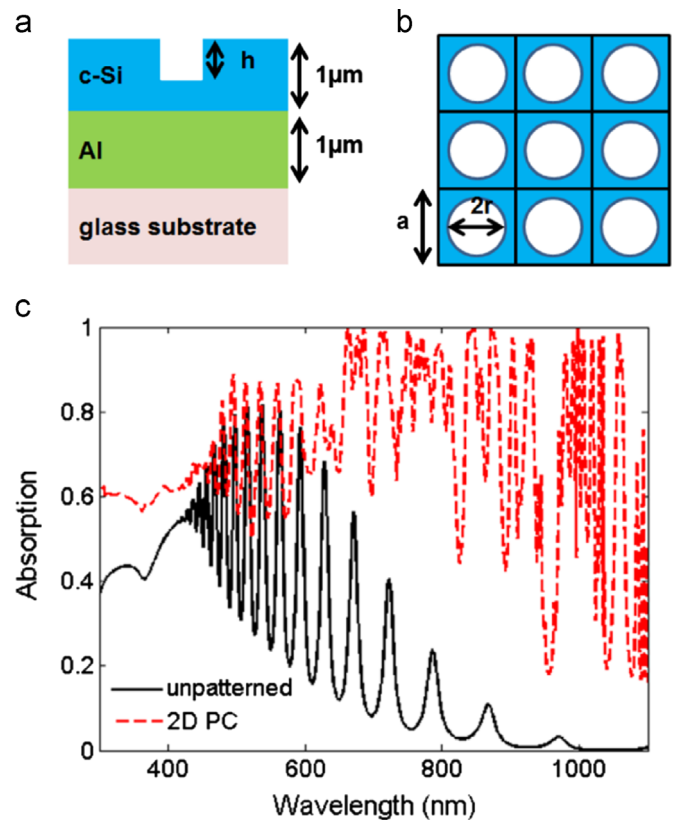


Fig. 1. (a) A patterned thin (c-Si) film lies on a metallic layer bonded on a glass substrate. (b) A square lattice (period a) of partially etched (etching depth h) hole (radius r) is used to increase the absorption of the stack. (c) Comparison between the absorption of the unpatterned thin film (black curve) and the absorption of the optimized photonic crystal structure (red dashed line). (For interpretation of the references to color in this figure legend, the reader is referred to the web version of this article.)

enhancement of the total absorption is chosen such as to be compared to the experimental values of the reflectance. Section 3 presents the experimental methods. The structures are realized thanks to Electron-Beam Lithography (EBL) and then optically characterized. Then in order to remove the influence of the back mirror, a preliminary experimental validation of our approach is obtained using a thin Silicon-On-Insulator (SOI) structure, this is discussed in Section 4. In addition even if not realistic at a larger scale, this stack exhibits an almost perfect flatness that can partly prevent from experimental deviations of the geometry. In Section 5, pseudo-disordered structures are realized in a thin c-Si film [24] and bonded on metal. The optical measurements performed on these structures are then analyzed in light of the numerical simulations.

2. Design and simulation results

Let us first consider a two-dimensional (2D) lattice of holes partially etched in a c-Si layer bonded on Aluminum on glass, as depicted in Fig. 1a. Thanks to an in-house developed analytical Rigorous Coupled Wave Analysis (RCWA) code, we compute the absorption in the whole stack. The number of orders used in the simulation and the wavelength step are chosen in order to achieve accurate numerical results. The incident light is an unpolarized plane wave at normal incidence. The figure-of-merit consists of the integrated absorption of the whole stack from 300 to 1100 nm (which corresponds to the relevant range of interest for c-Si solar cells), taking into account the solar spectrum [25].

A 2D square lattice of holes, as the one depicted in Fig. 1b, is characterized by its period (a), air filling factor in area ($ff = \pi r^2/a^2$) and the etching depth of the holes (h). The parameters resulting from the optimization of these 3 parameters are a period of 657 nm, a filling factor of 0.42 and an etching depth of 213.5 nm. These values are in good agreement with results obtained on a quite similar stack [22]. The resulting absorption spectrum is then plotted in Fig. 1c and compared to the absorption spectrum for the unpatterned case. Thanks to the PC structure, the integrated absorption is enhanced from 37.7%, in the unpatterned case, to 70.7%, this corresponds to a relative enhancement of 87.8%. As discussed in Section 1, this absorption is partly in the c-Si (integrated absorption of 39%) and in the metal (31.7%).

In order to further increase the absorption of this square lattice of holes, we introduce a controlled disorder in a 3×3 supercell. According to the well-known grating law, the resulting supercell period of $1.97 \mu\text{m}$ enables the diffraction of the impinging light all over the sunlight spectrum into at least the first order of all the guided modes in the c-Si film. It can be noted that this period of $1.97 \mu\text{m}$ is close to the period used for the quasi-random nanostructure in [22]. Such a mechanism, thanks to the rich Fourier spectrum of the dielectric function, has already shown its interest for light trapping. In our 3×3 supercell, all the holes are moved randomly from their position in the simply periodic structure. As depicted in Fig. 2a one hole is shifted by a distance d under an angle θ . The shift value d is determined thanks to a random Gaussian distribution defined by its mean value and its width value; while the angle value θ is determined randomly from 0° to 360° (uniform distribution). An example of a resulting pseudo-disordered structure for our selected 3×3 supercell is depicted in Fig. 2b. In order to prevent numerical and technological difficulties we restrict this study to situations where holes do not overlap.

As the simulations are based on a non-deterministic design (random values are used to move the hole) we use the protocol defined below. We choose different mean value for the shift parameter d . It can be noted that the higher this value, the higher the perturbation of the periodic pattern is. For each selected value of mean shift, we simulated 10 different structures. As we selected 5 different values for the mean shift from 25 nm to 75 nm we computed the integrated absorption for 50 different structures, which correspond to different realizations of the disorder. The integrated absorptions calculated for all these structures are plotted in Fig. 2c.

These results clearly show that a pseudo-disordered structure can absorb more light than the optimized square lattice of holes. Let us first focus on the evolution of the averaged integrated absorption (black dashed line in Fig. 2(c)). When the value of d increases from 25 to 38 nm, the averaged integrated absorption increases from 71.8% to 72.0%. Then, this figure-of-merit remains quite constant for mean shift values from 38 to 63 nm. If the mean shift value is larger than 63 nm, the mean integrated absorption decreases down to 71.5%. This evolution of the mean integrated absorption is related to the range of integrated absorption that can be obtained as depicted by the black dots. When the value of d increases from 25 to 75 nm, the range of available integrated absorption extends from 71.0% to 72.5%. It can be noted that the available range of integrated absorption increases with the value of d . This range grows up from 0.4% (for $d=25$ nm) to more than 1% (for $d > 63$ nm). Such a behavior is directly linked to the distance between holes that can strongly change in the case of high d value. It appears that pseudo-disordered structures that exhibit low integrated absorption for high d values show cluster of holes that cannot be obtained with low d values.

As the reference structure in this study is an optimized square lattice of holes, the amount of disorder introduced in the lattice should be carefully chosen. Designs including highly perturbed

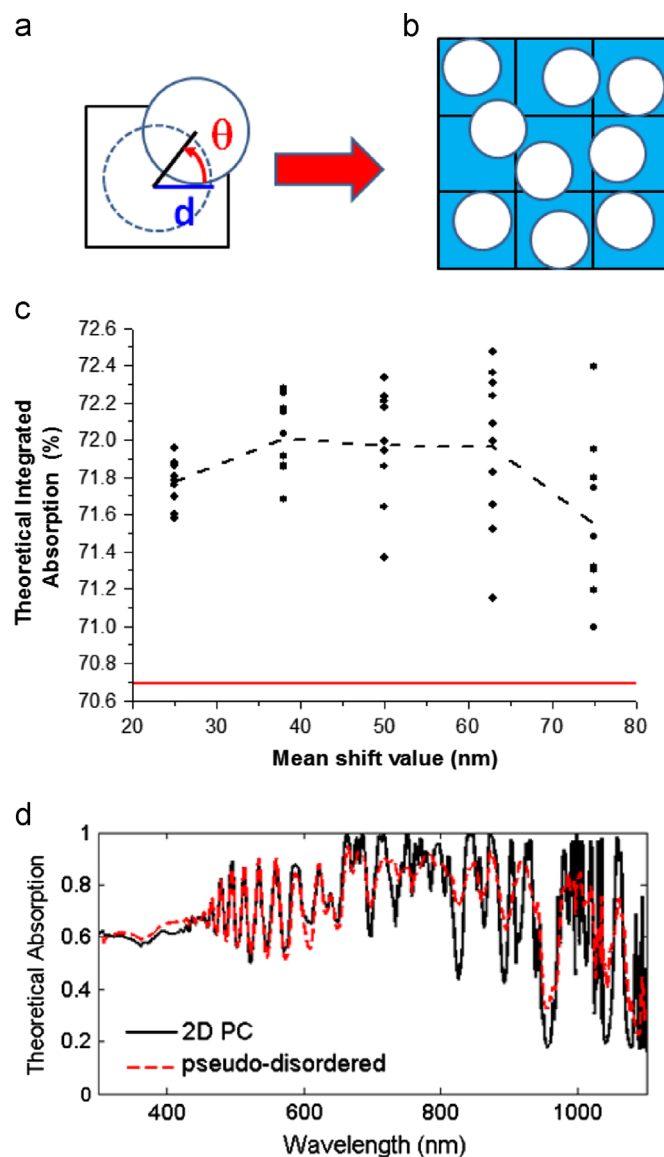


Fig. 2. (a) One hole is shifted of a distance d from its original position with an angle θ . (b) For a 3×3 supercell 9 holes are moved randomly leading to pseudo-disordered structure. (c) Evolution of the theoretical integrated absorption for several pseudo-disordered structure (dark dot). The mean value of integrated absorption (black dashed line) remains higher than the reference value (red horizontal line). (d) Comparison between the theoretical absorption of optimized photonic crystal structure (black curve) and the theoretical absorption of the best pseudo-disordered structure (red dashed line). (For interpretation of the references to color in this figure legend, the reader is referred to the web version of this article.)

patterns could lead to a decrease of the integrated absorption compared to a slightly pseudo-disordered structure. Indeed, the gain at large wavelengths can be lost by a poor absorption at low wavelengths, due to a far lower diffraction efficiency than using the square lattice of holes.

Let us now focus on the best pseudo-disordered structure which corresponds to an optimized design. For this selected structure, the expected integrated absorption reached is as high as 72.5%, which corresponds to an absolute increase of 1.8% (and a relative enhancement of 2.6%) compared to the previously optimized square lattice of holes structure. The absorption spectra corresponding to these 2 structures are plotted in Fig. 2c. Even if the pseudo-disordered structure appears to have less absorption peaks than the optimized square lattice of hole, this structure exhibits more modes thanks to the introduced perturbation, as

expected from previous theoretical work [17,18]. As the amplitude of these peaks is small, the result is a broadening of the peaks and then the number of visible peaks decreases.

Based on this theoretical investigation and considering the need to accurately control the position of the holes, the next section of the manuscript is dedicated to the nanofabrication process and optical characterization of the realized structures.

3. Fabrication process and measurement methodology

In this section we focus on the realization and characterization of pseudo-disordered structures. As the pseudo-disordered PC are defined at the nanometric scale (in size as well as in position of the holes), the lithography technique requires a high resolution and a large flexibility. So we resort to Electron Beam Lithography (EBL).

The process-flow required to realize these model structures as depicted in Fig. 3a–d. The first step is the nanophotonic structures patterning in a thin PMMA resist deposited on top of the considered stack. In order to reduce the lithography time, the size of the patterned area is limited to $100 \times 100 \mu\text{m}^2$. The PMMA is then transferred into the SiO_2 layer by Reaction Ion Etching using CHF_3 , and then to c-Si, using a SF_6 :Ar mixture. In order to ensure vertical sidewalls these 2 etching steps are performed at a low pressure. The remaining part of the SiO_2 layer is kept on top of the Si patterns, so as to mimic the anti-reflective coating which will be present on top of a final device. An example of a realized structure is shown on Fig. 3e.

Due to the limited size of the patterned area, the well-established integrating sphere measurement method cannot be used to determine the absorption of our thin patterned film. Thus we will resort to a micro-reflectivity set-up. In order to be as close as possible to the numerical incident light (plane wave at normal

incidence) the area of the pattern should then be as large as possible.

A schematic view of the micro-reflectivity set-up used to optically characterize the structures is depicted on Fig. 4. A nearly collimated white light is focused onto the nanopatterned structure through a long-focal microscope objective. The back reflection of the structure is collected through the objective lens and then analyzed using a spectrometer.

4. Silicon-On-Insulator-based pseudo-disordered absorbers

We first consider a simple model structure based on a Silicon-On-Insulator (SOI) wafer (Fig. 5a). With this simple structure, we focus on the c-Si absorbing layer, without considering the back metal and its parasitic absorption [8]. In addition, in such a wafer, the layers exhibits low roughness (less than 1 nm in rms) and allows the realization of nanopatterned which topography is quite close the designed PC structure. As we will use this kind of structures as model structures, we selected to perform the realization of two optimized structures: the pseudo-disordered structure that exhibits the highest absorption and the square lattice of holes that will be used as a reference. Lastly, we choose to limit the size of the patterned area to $300 \times 300 \mu\text{m}^2$, which is a trade-off between the time needed to realize the structure and the mismatch between optical simulation and characterization.

In the case of the square lattice of holes, let us then compare the theoretical reflection spectrum (obtained with a plane wave under normal incidence) plotted in Fig. 5b and the experimental one plotted in Fig. 5d. In the short wavelength range (below 800 nm) the experimental reflection is lower than the theoretical one. The lower experimental reflection is mainly due to the collection angle of the objective which does not collect efficiently the diffracted light in the first order at wavelengths smaller than the

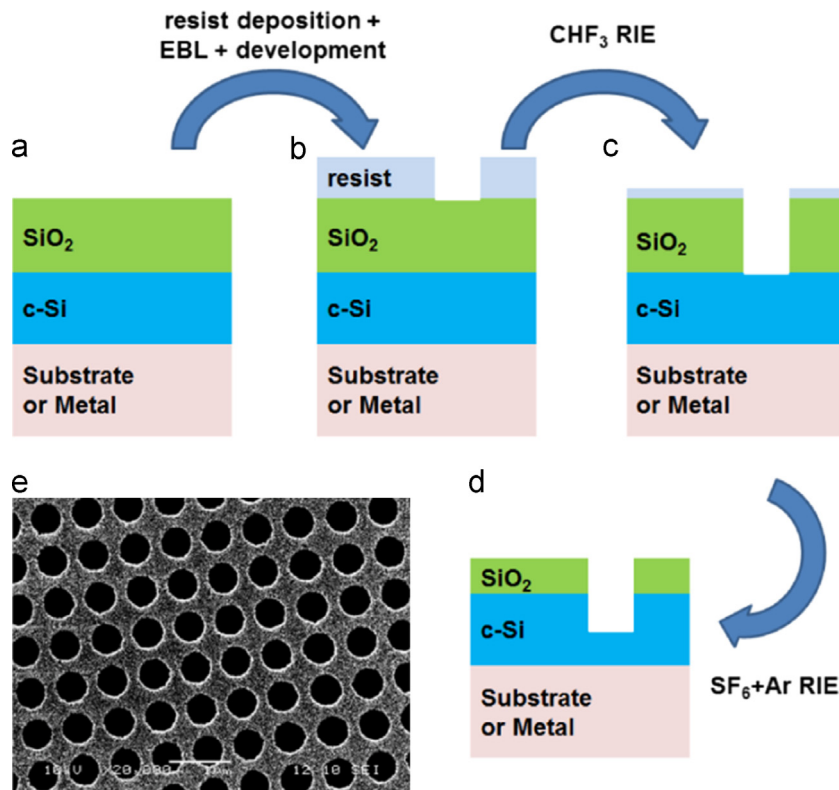


Fig. 3. Process flow to obtain the desired structure. On a SOI stack (a) EBL is used to imprint the design of the structure (b). Then 2 steps of RIE at low pressure (c–d) are used to transfer the design in the c-Si layer. (e) SEM view of a structure.

period. As it can be seen the specular reflection for wavelength shorter than the period of the photonic crystal almost corresponds to the experimental reflection. For the long wavelength range (from 800 to 1000 nm, which corresponds the highest achievable wavelength of our spectrometer) the sharp peaks displayed in the simulated spectrum (corresponding to high quality factor optical resonances) cannot be observed experimentally. In order to increase the agreement between the experimental spectrum and the theoretical one for wavelength larger than 800 nm, we should take into account the profile of the incident light. Indeed, in experiments, the structures are not illuminated by a plane wave, but by a Gaussian beam profile. Thanks to the $300 \times 300 \mu\text{m}^2$ size of the structure small magnification objectives ($\times 5$) can be used, with a corresponding numerical aperture of 0.14. In simulations, the plane wave under normal incidence usually used in RCWA is then replaced by a summation of plane waves under different angle that mimic the experimental Gaussian beam incident on the structure [26]. Such a substitution increases the computational time by a factor directly proportional to the number of plane waves used in the summation. Thus such simulations can be performed within a reasonable time only for the square lattice of

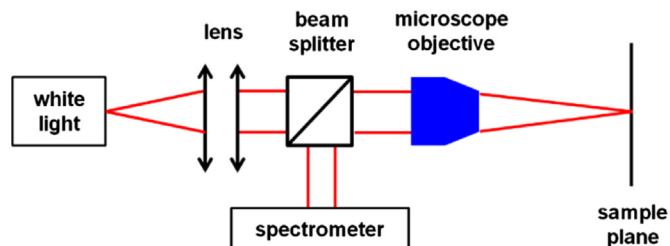


Fig. 4. (a) Micro-reflectivity set-up. A white light is focused on the nanostructure thanks to a long working distance objective. The back-reflection of the structure is analyzed through a spectrometer.

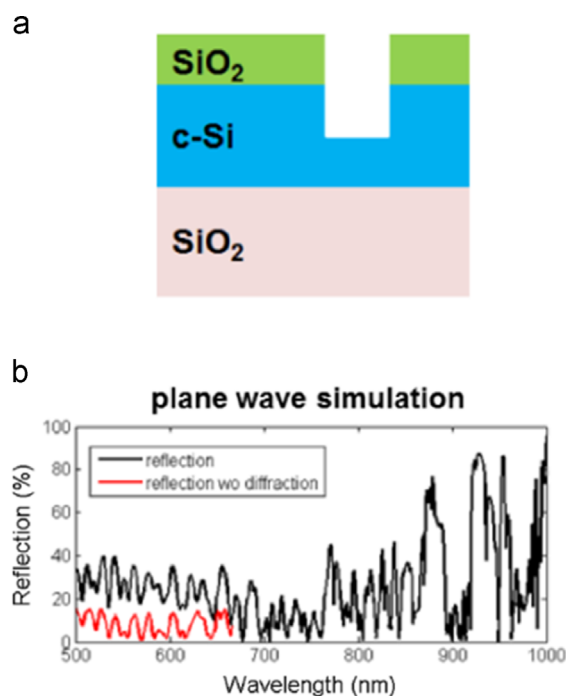


Fig. 5. (a) The square lattice of hole is patterned into the depicted SOI stack. In order to achieve a good agreement at large wavelengths between experiment and simulation, the usual theoretical reflection spectrum (obtained for a plane wave under incidence) (b) is replaced by the reflection spectrum obtained for a Gaussian beam under normal incidence (c) that mimic the experimental incident light used to obtain the experimental reflection spectrum (d). The red line in (b) corresponds to the specular reflection for wavelength smaller than the period of the photonic crystal. (For interpretation of the references to color in this figure legend, the reader is referred to the web version of this article.)

holes. Let us now compare the theoretical spectrum obtained with the Gaussian beam simulation (Fig. 5c) with the experimental spectrum (Fig. 5d). For the long wavelength range (from 800 to

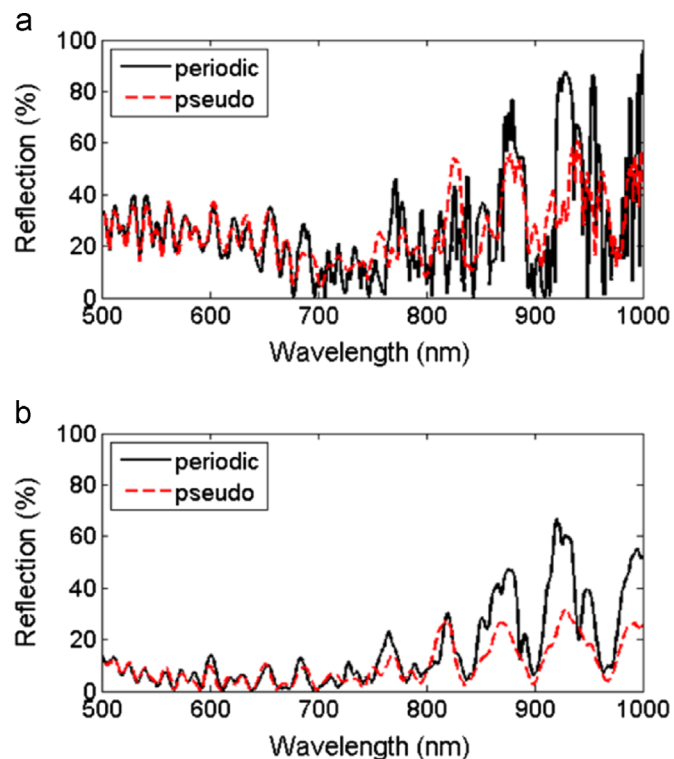
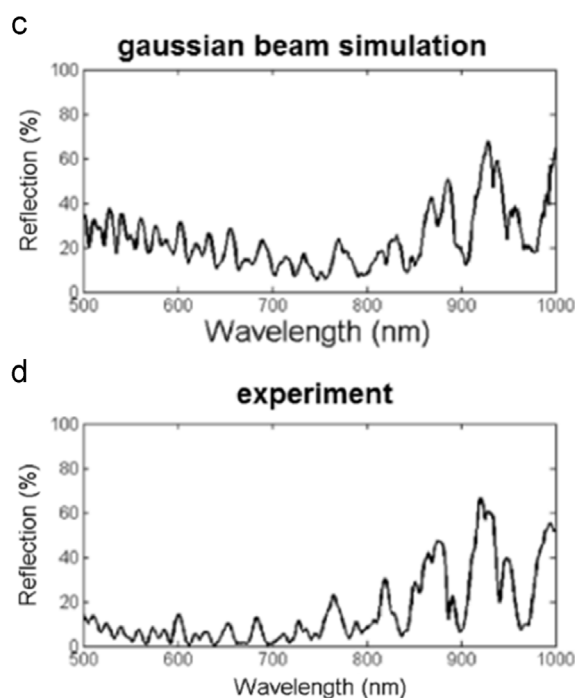


Fig. 6. Comparison between reflection theoretical (a) and experimental (b) reflection spectra obtained for the square lattice of holes (dark line) and for the pseudo-disordered structure (red dash line). (For interpretation of the references to color in this figure legend, the reader is referred to the web version of this article.)



1000 nm) the number of peaks, the quality factor and their contrast are in much better agreement. However for the wavelength range between 650 and 800 nm while the positions of peaks match well, their maxima somehow disagree. This difference is probably due to the collection of light (limited to the specular reflection) and to the roughness (≈ 1 nm in rms) of the remaining SiO_2 layer.

In order to study the effect of the pseudo-disordered structure, we limit the simulation to the case of a plane wave at normal incidence to compute the absorption of our thin layer with or without disorder, as depicted in Fig. 6a. As theoretically expected (Fig. 6a) for wavelengths below 700 nm, the pseudo-disordered structure and the square lattice of holes exhibit almost the same experimental reflection spectra (Fig. 6b). As these spectra (square lattice and pseudo-disordered structure) should almost be the same theoretically, we can conclude that the designed pseudo-disorder should not affect the absorption for these wavelengths.

For wavelengths above 700 nm, some of the sharp peaks visible on the theoretical spectrum of the square lattice of holes are broadened on the pseudo-disordered structure spectrum. The expected high quality factor peaks in the pseudo-disordered case are related to the limited diffraction efficiency of the incident plane wave into the added orders [17], even if their intensity can be small. However, as the experimental incident light is a Gaussian beam, the coherence of this light is lower than the coherence of the theoretical plane wave. Thus these high quality factor peaks are not visible on the experimental spectra shown in Fig. 6b. For the wavelengths between 700 and 1000 nm, the experimental reflection of the pseudo-disordered structure is almost always lower than the experimental reflection of the square lattice of holes which implies that the pseudo-disordered structure provides a better enhancement than the ordered one. Finally, a broadening of the absorption peak is visible near 875 and 925 nm on the experimental absorption spectrum, in the case of the pseudo-disordered structure. Thus the pseudo-disordered structure exhibits a significantly higher absorption than the square lattice of holes as expected theoretically.

Let us summarize the results obtained on these model structures. The experimental spectra are in good agreement with the theoretical ones (as calculated for a Gaussian profile incident light). As expected theoretically, introducing a pseudo-disorder does not change the reflection at the short wavelengths. However, for the short wavelength range, the discrepancies between the numerical spectrum and the experimental one are mainly due to the limited collection angle (first diffracted order are experimentally measured) and to experimental fluctuations (in particular the surface roughness and the circularity of holes). In the long wavelength range, the discrepancies between the illumination condition in the numerical and experimental cases (mainly Gaussian beam vs plane wave), and also considering the remaining roughness and non-uniformities of the pattern in the fabricated structures, the reflection spectra exhibit broadened peaks which could artificially increase the measured integrated absorption. Still, introducing a pseudo-disorder in a simply periodic PC does lead to a reflection decrease in the long wavelength range. Taking into account these remarks, we will now investigate the effect of pseudo-disorder in the case of a thin c-Si layer bonded onto a metal layer standing on a glass substrate.

5. c-Si-on-metal pseudo-disordered structures

We consider the stack depicted in Fig. 1a, including a $1 \mu\text{m}$ thick c-Si layer standing on an Al layer. Using the process-flow presented in the previous section (Fig. 3), we realize all the structures simulated in and presented in Section 2. As a large number of

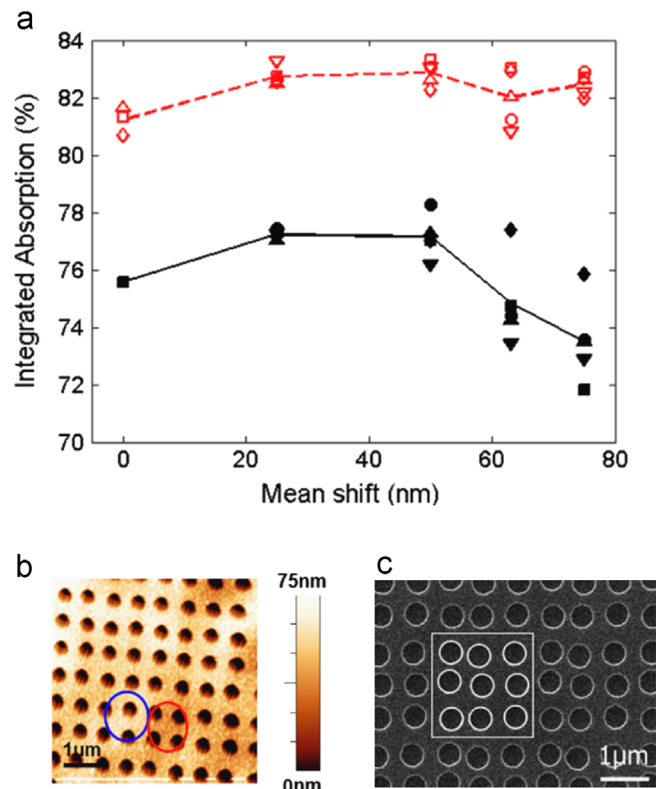


Fig. 7. (a) Evolution of the mean integrated absorption experimentally (red dash line) and theoretically (black line). The filled symbols (unfilled symbols) correspond to measurement (simulation) of integrated absorption for different pseudo-disordered structure. The reference value for the square lattice of holes corresponds to a mean shift value of 0 nm. AFM (b) and SEM (c) view of a realized structure. (For interpretation of the references to color in this figure legend, the reader is referred to the web version of this article.)

structures have to be fabricated by EBL, the size of each structure was reduced to $100 \times 100 \mu\text{m}^2$. This size is chosen in order to nanopattern all the structures in a single run of EBL, limiting discrepancies and experimental fluctuation.

As mentioned in the previous part of this manuscript, the pseudo-disorder should not lead to an increase of the absorption in the low wavelength range of the spectrum, compared to the square lattice of hole. Therefore, we calculate the integrated absorption for all the structures within the 700–1000 nm range, always taking into account the solar spectrum. To make a fair comparison between results, we update the numerical results and compute the integrated absorption over the same spectral range. The experimental integrated absorption (81.2%) is higher than the expected theoretical one (75.6%) for the square lattice of holes structure (Fig. 7a). It can be noted that 3 different experimental values are presented for the square lattice of holes. The spread of the values is related to geometrical imperfections; it remains limited compared to the effect of the pseudo disorder.

Then we compute the mean value of the integrated absorption for the different experimental pseudo-disordered structures. The gain on this averaged optical absorption is also displayed on Fig. 7a. Although the experimental absorption overpasses the theoretical one (Fig. 7a), these two curves exhibit almost the same behavior. First the integrated absorption increases experimentally as well as theoretically with the mean shift value. Then the mean absorption decreases for higher mean shift value. The main difference between the 2 curves appears in the case of the highest mean shift value, which does not decrease in the experiments. On the same plot we add the integrated absorption of the 5 structures closest to the average. As the mean shift value increases, the

available range for the integrated absorption increases experimentally as well as theoretically for the highest experimental mean shift.

Even if the average value of the measured optical absorption is 5.7% higher than the simulated one, the maximal enhancements of the averaged value due to the pseudo-disorder are quite comparable in the experiments and simulation (around 1.7% in absolute value). For the best pseudo-disordered structure, the experimental integrated absorption increases by 2.1% compared to the square lattice of holes which a little bit less than the theoretical increases of 2.7%.

Let us now consider the offset of integrated absorption between theoretical and experimental results (+5.7%). The Atomic Force Microscope (AFM) view plotted in Fig. 7b clearly shows the roughness of the realized structure. First, the roughness of the thin c-Si film on metal is significantly higher than the roughness of the previous SOI wafer. For instance, the peak-to-valley highlighted by circle spots exhibit a topographical difference of ≈ 10 nm. In addition the remaining SiO₂ layer exhibits a smaller-scale roughness due to the RIE etching (roughness of ≈ 1 nm). In addition, on the SEM view of Fig. 7c, one can notice that the circular shape of holes exhibit a small roughness. Moreover, as the size of the patterned area decreases from $300 \times 300 \mu\text{m}^2$ to $100 \times 100 \mu\text{m}^2$ we used a higher magnification microscope objective, which results in a discrepancy increase between the experimental and the theoretical illumination conditions. Altogether, this leads to a higher difference between experimental and theoretical spectra compared to the previous measurements on a patterned SOI wafer. In particular, the expected high quality factor peaks of the theoretical absorption spectrum cannot be obtained experimentally. Lastly, for the shortest wavelengths, the experimental reflection of the structure is far below the one expected from the simulation. Thus the integrated absorption from the experiment is substantially higher than the theoretical one.

Let us now sort and summarize the reasons for the differences between experimental results and simulations. The reasons can be attributed to nanopatterning imperfections (sidewall roughness, etching depth profile, etc.) like in the case of the patterned SOI structure but also material characteristics (e.g., interface roughness, contamination of c-Si by the Al back layer) and discrepancy between numerical and experimental illumination conditions (in particular, plane wave/Gaussian beam, spatial homogeneity of the beam). Despite these differences, we highlight that the experimental integrated absorption exhibits almost the same behavior as the theoretical one. Thanks to our perturbative approach, we evidence that the magnitude of the introduced disorder exhibits an optimum around a specific mean shift value. Thanks to the square lattice of holes structure patterned into the thin c-Si layer, the integrated absorption increases almost by a factor of 2 compared to the flat reference. Replacing the optimized square lattice of holes by the optimized pseudo-disordered structure, which can be achieved keeping the same process to realize the nanopattern, increases experimentally as well as theoretically the integrated absorption by 2%. This absolute increase of 2% can be achieved at almost no extra technological cost, provided a reliable replication method is used. For instance, the master stamp of nanoimprint lithography can be realized in the same way for a square lattice of holes and for a pseudo-disordered structure.

6. Conclusion

Using RCWA simulation, we introduced a solar cell design based on a $1 \mu\text{m}$ thick c-Si layer standing on a Al layer, patterned as an optimized photonic crystal including a controlled disorder. This as expected led to an almost two-fold increase of the optical

absorption, over a broad and relevant wavelength range. The integrated absorption enhancement overpasses that expected using a fully optimized square lattice photonic crystal pattern, while its fabrication can be achieved using exactly the same process. In order to further demonstrate the interest of these complex nanophotonic patterns, experiments were performed on simply periodic and pseudo-disordered nanopatterns. Model structures were first patterned in a Silicon-On-Insulator wafer, in order to highlight the influence of experimental fluctuations related to the process imperfections, and the impact of the illumination conditions on the expected absorption spectra. Technological imperfections mainly increase the optical absorption in the active c-Si layer at the shortest wavelengths of the solar spectrum. Then selected pseudo-disordered patterns have been patterned in a thin c-Si film bonded on top of the metal layer. The experimental integrated absorption measured in this solar cell stack almost exhibits the same behavior as the theoretical one, despite a constant offset. Compared to a simply periodic photonic crystal, the best pseudo-disordered structure enhanced the overall optical absorption up to 2.1% which is in good agreement with the 2.7% increase expected theoretically.

The optical study involved in this work will be further extended to the case of a fully functional solar cell, enabling electro-optical characterization. As the considered stack in this work is closed to a realistic c-Si solar cell stack, even if the design modification will be limited, a new optimization should be done by taking into account only the absorption in the active layer (e.g. without the parasitic absorption in electrode). It remains that expected relative enhancements of the absorption in (c-Si) should be of the same order of magnitude than in the whole stack. Indeed, the pseudo disorder pattern does not change significantly the vertical distribution of the optical modes. The remaining challenge stands in the fabrication of nanopatterns over square centimeters. To obtain such large scale patterns one can resort to High-Voltage EBL (at least 100 kV) in order to achieve high lithography speed without losing at the resolution of the structure. For a widespread use of pseudo-disordered patterns, such an EBL is only required to fabricate a large master stamp, that will be replicated using Nanoimprint Lithography, as it has been already done at a smaller scale [27].

Acknowledgments

The authors acknowledge Pierre Cremillieu and Radoslaw Mazurczyk for their efficient support on the NanoLyon technological platform, Cécile Jamois and Aurélien Griffart for their help on optical characterization. The research leading to these results has received funding from the European Union Seventh Framework Programme under grant agreement no. 309127 (PhotoNVoltaics). H.D. acknowledges the China Scholarship Council (CSC). This work is funded by the French Research Agency (Grant no. ANR-12-PRGE-0004) program (Nathisol).

Appendix

The refractive indices and extinction coefficients used in the optical simulation and corresponding to (c-Si) [28] and Al [29] are displayed in Fig. 8.

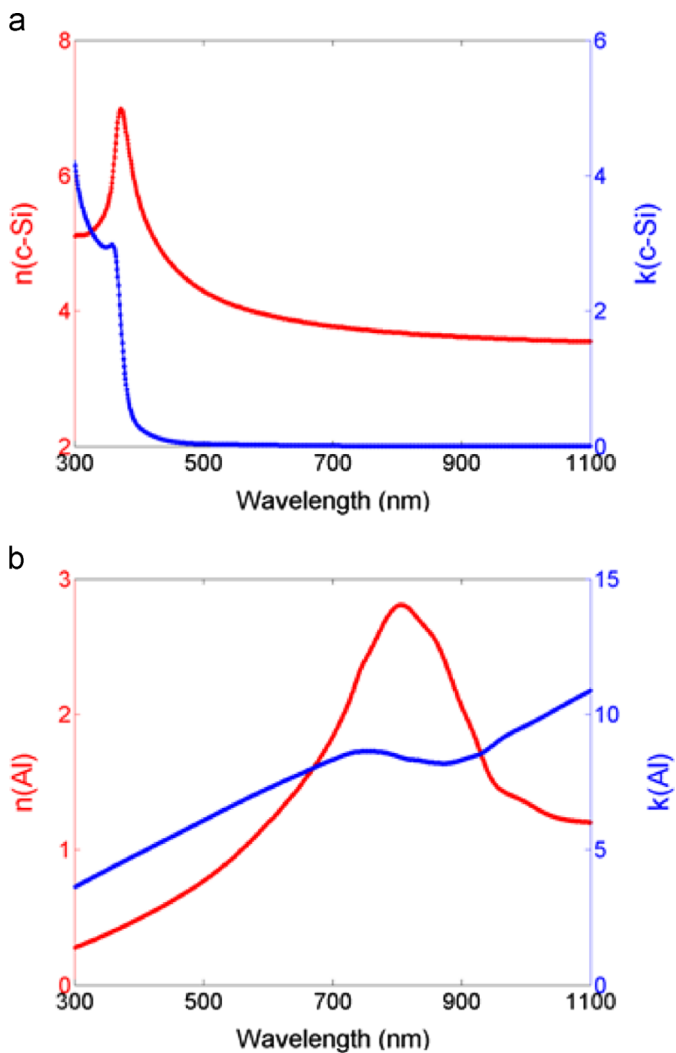


Fig. 8. Optical indexes used in the simulations for the (c-Si). (a) and the Al (b). The refractive index (n) is plotted in red while the extinction coefficient (k) is plotted in blue. (For interpretation of the references to color in this figure legend, the reader is referred to the web version of this article.)

References

- [1] J.G. Mutitu, S. Shi, C. Chen, T. Creazzo, A. Barnett, C. Honsberg, D.W. Prather, Thin film solar cell design based on photonic crystal and diffractive grating structures, *Opt. Express* 16 (19) (2008) 15238–15248.
- [2] P. Spinelli, V.E. Ferry, J. van de Groep, M. van Lare, M.A. Verschuuren, R.E. I. Schropp, H.A. Atwater, A. Polman, Plasmonic light trapping in thin-film Si solar cells, *J. Opt.* 14 (2) (2012) 024002–1–024002–11.
- [3] C.S. Schuster, S. Morawiec, M.J. Mendes, M. Patrini, E.R. Martins, L. Lewis, I. Crupi, T.F. Krauss, Plasmonic and diffractive nanostructures for light trapping – an experimental comparison, *Optica* 2 (3) (2015) 194–200.
- [4] G. Gomard, E. Drouard, X. Letartre, X. Meng, A. Kaminski, A. Fave, M. Lemiti, E. Garcia-Caurel, C. Seassal, Two-dimensional photonic crystal for absorption enhancement in hydrogenated amorphous silicon thin film solar cells, *J. Appl. Phys.* 108 (12) (2010) 123102.
- [5] X. Meng, V. Depauw, G. Gomard, O. El Daif, C. Trompoukis, E. Drouard, C. Jamois, A. Fave, F. Dross, I. Gordon, C. Seassal, Design, fabrication and optical

- characterization of photonic crystal assisted thin film monocrystalline-silicon solar cells, *Opt. Express* 20 (s4) (2012) A465–A475.
- [6] M.S. Branham, W.C. Hsu, S. Yerci, J. Loomis, S.V. Boriskina, B.R. Hoard, S.E. Han, G. Chen, 15.7% efficient 10- μm -thick crystalline silicon solar cells using periodic nanostructures, *Adv. Mat.* 27 (2015) 2182–2188.
- [7] S. Jeong, M.D. Mc Gehee, Y. Cui, All-back-contact ultra-thin silicon nanocone solar cells with 13.7% power conversion efficiency, *Nat. Commun.* 4 (2013) 2950.
- [8] V. Depauw, X. Meng, O. El Daif, G. Gomard, L. Lalouat, E. Drouard, C. Trompoukis, A. Fave, C. Seassal, I. Gordon, Micrometer-thin crystalline-silicon solar cells integrating numerically optimized 2-D photonic crystals, *IEEE J. Photovolt.* 4 (2014) 215–223.
- [9] C.S. Schuster, P. Kowalczewski, E.R. Martins, M. Patrini, M.G. Scullion, M. Liscidini, L. Lewis, C. Reardon, L.C. Andreani, T.F. Krauss, Dual gratings for enhanced light trapping in thin-film solar cells by a layer-transfer technique, *Opt. Express* 21 (S3) (2013) A433–A438.
- [10] X. Meng, E. Drouard, G. Gomard, R. Peretti, A. Fave, C. Seassal, Combined front and back gratings for broad band light trapping in thin film solar cell, *Opt. Express* 20 (S5) (2012) A560–571.
- [11] Y. Tanaka, Y. Kawamoto, M. Fujita, S. Noda, Enhancement of broadband optical absorption in photovoltaic devices by band-edge effect of photonic crystals, *Opt. Express* 21 (17) (2013) 20111–20118.
- [12] K. vynck, M. Burresi, F. Riboli, D.S. Wiersma, Photon management in two-dimensional disordered media, *Nat. Mater.* 11 (2012) 1017–1022.
- [13] C. Battaglia, C.M. Hsu, K. Söderström, J. Escarré, F.J. Haug, M. Charrière, M. Boccard, M. Despeisse, D.T.L. Alexander, M. Cantoni, Y. Cui, C. Ballif, Light trapping in solar cells: can periodic beat random? *ACS Nano* 6 (3) (2012) 2790–2797.
- [14] R.A. Pala, J.S.Q. Liu, E.S. Barnard, D. Askarov, E.C. Garnett, S. Fan, M. L. Brongersma, *Nat. Commun.* 4 (2013) 2095.
- [15] J. Xavier, J. Probst, F. Back, P. Wyss, D. Eisenhauer, B. Löchel, E. Rudigier-Voigt, C. Becker, Quasicrystalline-structures light harvesting nanophotonic silicon films on nanoimprinted glass for ultra-thin photovoltaics, *Opt. Mater. Exp.* 4 (11) (2014) 2290–2299.
- [16] H. Ren, Q.G. Du, F. Ren, C.E. Png, Photonic quasicrystal nanopatterned silicon thin film for photovoltaic applications, *J. Opt.* 17 (2015) 035901.
- [17] R. Peretti, G. Gomard, L. Lalouat, C. Seassal, E. Drouard, Absorption control in pseudodisordered photonic-crystal thin films, *Phys. Rev. A* 88 (2013) 053835.
- [18] A. Oskooi, P.A. Favuzzi, Y. Tanaka, H. Shiget, Y. Kawakami, S. Noda, Partially disordered photonic-crystal thin films for enhanced and robust photovoltaics, *Appl. Phys. Lett.* 100 (2012) 181110.
- [19] C. Lin, L.J. Martinez, M.L. Povinelli, Experimental broadband absorption enhancement in silicon nanohole structures with optimized complex unit cells, *Opt. Exp.* 21 (S5) (2013) A872–A882.
- [20] U.W. Paetzold, M. Smeets, M. Meier, K. Bittkau, T. Merdzhanova, V. Sirnov, D. Michaelis, C. Waechter, R. Carius, U. Rau, Disorder improves nanophotonic light trapping in thin-film solar cells, *Appl. Phys. Lett.* 104 (2014) 131102.
- [21] A. Bozzola, M. Liscidini, L.C. Andreani, Broadband light trapping with disordered photonic structures in thin-film silicon solar cells, *Prog. Photovolt.: Res. Appl.* 12 (2014) 1237–1245.
- [22] E.R. Martins, J. Li, Y. Liu, V. Depauw, Z. Chen, J. Zhou, T.F. Krauss, Deterministic quasi-random nanostructures for photon control, *Nat. Commun.* 4 (2013) 2665.
- [23] M.G. Moharam, E.B. Grann, D.A. Pommet, T.K. Gaylord, Formulation for stable and efficient implementation of the rigorous coupled-wave analysis of binary gratings, *J. Opt. Soc. Am. A* 12 (5) (1995) 1068–1076.
- [24] V. Depauw, Y. Qiu, K. Van Nieuwenhuysen, I. Gordon, J. Poortmans, Epitaxy-free monocrystalline silicon thin film: first steps beyond proof-of-concept solar cells, *Prog. Photovolt.: Res. Appl.* 19 (2010) 844–850.
- [25] AM1.5 Reference Solar Spectrum, (<http://rredc.nrel.gov/solar/spectra/am1.5/>).
- [26] S.D. Wu, T.K. Gaylord, E.N. Glytsis, Y.M. Wu, Three-dimensional converging-diverging Gaussian beam diffraction by a volume grating, *J. Opt. Soc. Am. A* 22 (7) (2005) 1293–1303.
- [27] C. Trompoukis, O. El Daif, V. Depauw, I. Gordon, J. Poortmans, Photonic assisted light trapping integrated in ultrathin crystalline silicon solar cells by nanoimprint lithography, *Appl. Phys. Lett.* 101 (2012) 103901.
- [28] C. Herzinger, B. Johs, W. McGahan, J. Woollam, W. Paulson, Ellipsometric determination of optical constants for silicon and thermally grown silicon dioxide via a multi-sample, multi-wavelength, multi-angle investigation, *J. Appl. Phys.* 83 (1998) 3323–3336.
- [29] E.D. Palik, *Handbook of Optical Constants of Solids*, vol. 3, Academic Press, Cambridge, 1998.